Joule

CellPress

Article

Continuous hydrodeoxygenation of lignin to jet-range aromatic hydrocarbons

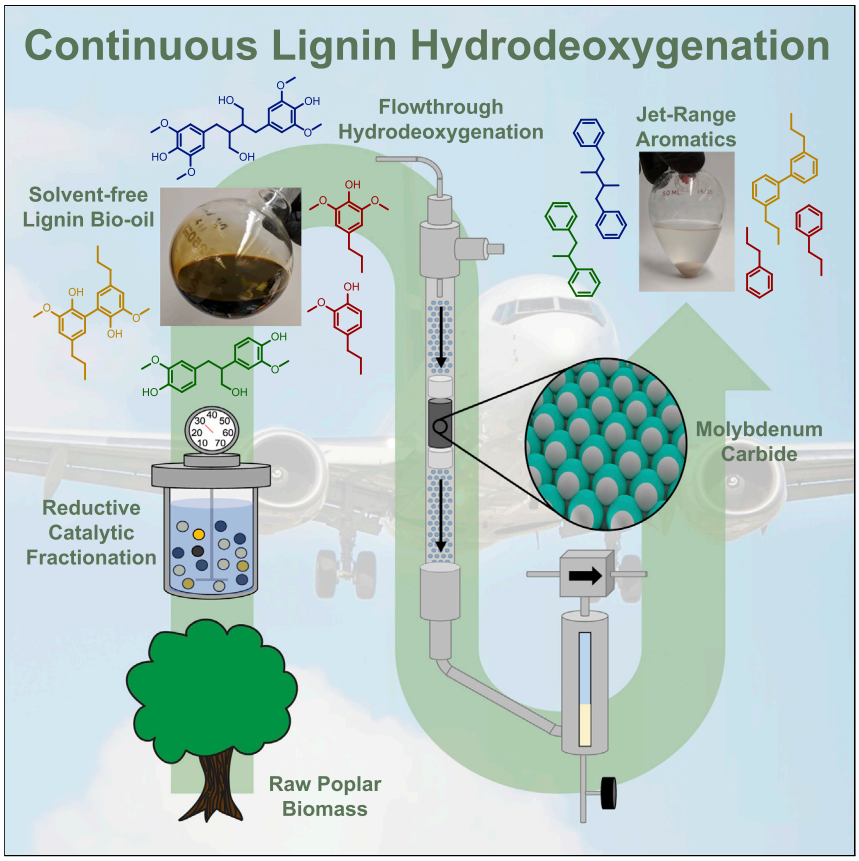

Processes that can generate high volumes of sustainable aviation fuels (SAFs) are essential to meet air travel demand while eliminating carbon emissions. Lignin is an abundant and renewable aromatic biopolymer that comprises 15%–30% of all lignocellulosic biomass but remains underutilized due to its chemical recalcitrance. Herein, we present a method for the conversion of lignin to jet-range aromatic hydrocarbons with high atom economy using a molybdenum carbide hydrodeoxygenation catalyst. The resulting products feature favorable properties for use in aviation fuel.

Michael L. Stone, Matthew S. Webber, William P. Mounfield III, ..., Joshua S. Heyne, Gregg T. Beckham, Yuriy Román-Leshkov

gregg.beckham@nrel.gov (G.T.B.)
yroman@mit.edu (Y.R.-L.)

Highlights

Stable deoxygenation of real lignin achieved with high aromatic selectivity

Two-pass flow-through HDO enables improved deoxygenated dimer yields

Deep lignin deoxygenation yields promising aromatic blendstock for use in SAF

Tier α characterization suggests performance-enhanced products

Stone et al., Joule 6, 1–14
October 19, 2022
https://doi.org/10.1016/j.joule.2022.08.005

Please cite this article in press as: Stone et al., Continuous hydrodeoxygenation of lignin to jet-range aromatic hydrocarbons, Joule (2022), https://doi.org/10.1016/j.joule.2022.08.005

Joule

CellPress

Article

Continuous hydrodeoxygenation of lignin to jet-range aromatic hydrocarbons

Michael L. Stone,[1] Matthew S. Webber,[1] William P. Mounfield III,[1] David C. Bell,[2] Earl Christensen,[3] Ana R.C. Morais,[3] Yanding Li,[1] Eric M. Anderson,[1] Joshua S. Heyne,[2,4] Gregg T. Beckham,[3,*] and Yuriy Román-Leshkov[1,5,*]

SUMMARY

Sustainable aviation fuel (SAF) is essential to decrease the carbon footprint of the aviation industry. Although many strategies have been developed to provide the linear and branched aliphatic components of SAF, few viable strategies have been demonstrated to supply the aromatic and cycloalkane fraction of the SAF at the necessary scale from bio-based feedstocks. Lignin is the largest natural source of renewable aromatic compounds; however, major challenges in deoxygenation have prevented its use as a feedstock for SAFs. Here, we report a continuous, two-stage catalytic process using molybdenum carbide to deoxygenate lignin from poplar into aromatic hydrocarbons with 87.5% selectivity toward aromatic hydrocarbons at 86% of the theoretical carbon recovery. Tier α fuel property testing indicates that the SAF-range lignin-derived aromatic compounds are likely performance-advantaged across multiple properties relative to conventional jet fuel aromatic compounds. This work demonstrates an effective approach to convert lignin into aromatic SAF blendstocks.

INTRODUCTION

In 2019, 106 billion gallons of jet fuel were consumed globally, and this number is expected to more than double by 2050 as a result of increased travel demand.[1] Meanwhile, to mitigate its impact on climate change, the aviation industry has pledged to achieve net carbon neutrality over the same time period.[2] To achieve this goal, sustainable aviation fuel (SAF) must be deployed at a massive scale. Today, most commercially available SAF is synthesized via deoxygenation of plant- and animal-derived lipid feedstocks to produce *iso*- and *n*-alkane hydrocarbon blends, but these feedstocks are not available in the volumes required to meet the projected fuel demand.[3–5] Notably, cycloalkanes and aromatics together comprise between 30 and 70 wt % of modern aviation fuel or between 32 and 74 billion gallons per year.[6,7] However, current ASTM-approved SAF technologies cannot produce the aromatic or the cycloalkane components at the scale necessary to satisfy the required properties of jet fuel (namely fuel density and elastomer compatibility) to power the existing fleet of aircrafts,[8,9] which is a constraint that has resulted in a 50% blending wall with conventional fossil fuels.[10] Although a number of technologies have attempted to address this challenge by generating both aromatics and cycloalkanes from syngas, lipid feedstocks, and cellulosic materials, so far none have been approved for use in SAFs without blending with conventional hydrocarbon fuels.[11,12] Nevertheless, technologies capable of generating both aromatics and cycloalkanes from abundant, renewable feedstocks

CONTEXT & SCALE

Decarbonization strategies for transportation are essential to curb climate change spurred by the use of fossil fuels. Although electrification has shown promise toward reducing the carbon footprint of passenger vehicles, aviation remains dependent on hydrocarbon fuels due to their high energy density relative to even the most advanced battery technologies available today. As such, multiple processes for the generation of sustainable aviation fuels (SAFs) have recently been developed. However, due to their lack of aromatic molecules, they require blending with conventional fuels to achieve the necessary characteristics for their safe use. By using lignin, an abundant, renewable biopolymer that has traditionally been underutilized due to its chemical recalcitrance, an aromatic SAF blendstock could be generated. This work demonstrates a process by which lignin can be selectively converted to jet-range aromatics at unprecedented carbon yields, providing a path toward a 100% drop-in SAF.

Please cite this article in press as: Stone et al., Continuous hydrodeoxygenation of lignin to jet-range aromatic hydrocarbons, Joule (2022), https://doi.org/10.1016/j.joule.2022.08.005

are likely essential to the development of a viable 100% drop-in SAF to power the current fleet of aircrafts.[13]

Lignin is the largest source of renewable aromatics available in nature[14] comprising between 15% and 30% of lignocellulosic biomass. In principle, the 90 million dry-tons of lignin harvested in the United States in 2017 could generate 15 billion gallons of jet-range hydrocarbons based on carbon content.[14,15] By 2040, this value could increase to 63 billion gallons annually (>50% of current global demand), given projections on future lignin availability.[14,15] Despite its potential, lignin is currently either re-dispersed in the field or slated to be burned for low grade heat by the cellulosic ethanol and paper industries because lignin becomes highly recalcitrant when separated from the cellulose fibers in biomass.[16] Alternative lignin extraction methods that rely on reductive catalytic fractionation (RCF),[17–20] protection group chemistries,[21–23] or flow-through solvolysis[24] minimize re-condensation pathways, but the resulting lignin oils have high oxygen contents ranging between 27 and 34 wt %,[9] which must be reduced to <0.5% for use in jet fuel.[10,25]

To this end, significant progress has been made toward the development of lignin hydrodeoxygenation (HDO) catalysts.[9] Many studies have utilized bifunctional acid/metal catalyst systems to deoxygenate lignin-derived phenolics,[26–34] but only a specific subset of these materials have demonstrated the ability to selectively cleave aryl–oxygen bonds while preserving aromaticity.[35–43] Molybdenum carbide (Mo_2C) stands out as an earth-abundant catalyst capable of stably removing both methoxy and phenolic groups from lignin model compounds with over 90% selectivity toward aromatics.[44–48] However, efforts using Mo_2C to upgrade real bio-derived lignin substrates have not been as successful.[49–51] In general, the translation of promising catalysts to viable processing strategies with real lignin feedstocks has been hindered by major challenges, such as the complex reaction engineering needed for recalcitrant lignin substrates, the required use of expensive noble-metal catalysts, prevalent catalyst deactivation coupled with low deoxygenation efficiency when using real feedstocks, excessive hydrogen consumption due to ring hydrogenation and hydrocracking, and low carbon yields due to condensation/coking, hydrocracking to gaseous products, or the upgrading of only the monomeric fraction.[9,52]

Here, we directly address these challenges by demonstrating a solvent-free process for the HDO of poplar RCF lignin oil with near-quantitative carbon yields using earth-abundant Mo_2C catalysts. Continuous flow HDO experiments with real lignin feeds under solvent-free conditions were performed in a custom-built three-phase trickle bed reactor (supplemental experimental procedures; Figure S1). Poplar RCF lignin oil (details in supplemental experimental procedures) was chosen as an illustrative lignin substrate, with recent studies showing potential for commercial implementation of RCF in a lignin-first biorefinery.[53,54] The RCF process solvolytically extracts and catalytically depolymerizes lignin from whole biomass to produce an oxygenated aromatic oil consisting of ~50 wt % monomeric species and ~50 wt % carbon-carbon linked dimers and larger oligomers.[18,19,55] Accordingly, complete deoxygenation of RCF oil would generate a mixture rich in alkylated arenes ranging between C9 and C20, which is ideal for jet fuel blending.

RESULTS

Tracking deoxygenation of lignin RCF products with Mo_2C

The RCF oil used in this study was generated by heating a mixture of poplar wood (compositional analysis in Table S1), 5 wt % Ru/C catalyst, and methanol under 30 bar hydrogen gas to 225°C under rapid stirring for 3 h (full experimental details

[1]Department of Chemical Engineering, Massachusetts Institute of Technology, Cambridge, MA 02139, USA

[2]Bioproduct Sciences and Engineering Laboratory, School of Engineering and Applied Science, Washington State University, Richland, WA 99354, USA

[3]Renewable Resources and Enabling Sciences Center, National Renewable Energy Laboratory, Golden, CO 80401, USA

[4]Energy Processes and Materials Division, Energy and Environment Directorate, Pacific Northwest National Laboratory, Richland, WA 99352, USA

[5]Lead contact

*Correspondence: gregg.beckham@nrel.gov (G.T.B.), yroman@mit.edu (Y.R.-L.)

https://doi.org/10.1016/j.joule.2022.08.005

Please cite this article in press as: Stone et al., Continuous hydrodeoxygenation of lignin to jet-range aromatic hydrocarbons, Joule (2022), https://doi.org/10.1016/j.joule.2022.08.005

in supplemental experimental procedures). An average delignification extent of 68 ± 3 wt % was achieved (average and standard deviation of 4 batch RCF experiments). The reaction conditions were optimized to achieve complete conversion of β-O-4 ether linkages (based on heteronuclear single quantum coherence [HSQC] 2D-NMR analysis, Figure S2) and maximize the monomer yield of the oil (Figure S3). The isolated RCF oil contained a total monomer content of 52.1 ± 0.8 wt % (average and standard deviation across 4 batches of RCF oil), with the major monomeric components being propylsyringol (PS) (24.3 ± 0.8 wt %), propylguaiacol (PG) (13.2 ± 0.1 wt %), dihydrosinapyl alcohol (PS-OH) (8.6 ± 0.7 wt %), and dihydroconiferyl alcohol (PG-OH) (5.1 ± 0.5 wt %) (complete composition available in Table S2). Gel permeation chromatography (GPC) shows the non-monomer fraction of the oil contains both dimers and higher oligomers (Figure S4), and although the precise quantification of these larger species remains a significant challenge,[56,57] we used gas chromatography coupled with mass spectrometry (GC-MS) after trimethylsilyl derivatization to identify many of the dimeric species present in the oil (Figure S5). CHN/O analysis of 4 batches of RCF oil showed 65.44 ± 0.10% C, 7.93 ± 0.08% H, 0.19 ± 0.02% N, and 26.53 ± 0.16% O (by difference).

The complexity of lignin oil components and their deoxygenated products necessitates rigorous analytical methods to close mass balances accurately. Accordingly, we identified and quantified partially and fully deoxygenated monomers and dimers during HDO experiments using a feed consisting of 2 wt % RCF oil dissolved in toluene (Figures S6 and S7). Unsupported Mo_2C was used as the catalyst due to its ability to directly cleave C–O bonds in model aromatic oxygenate molecules without hydrogenating the aromatic rings.[37,44,58] Although Mo_2C has not been studied extensively for the deep deoxygenation of lignin oil, we hypothesized it could provide a route toward hydrogen-efficient deoxygenation with control over aromatic product selectivity. Figure 1A summarizes all the lignin-derived monomers quantified by GC with flame ionization detection (GC-FID) in this study (see Figures S8 and S9; Tables S3 and S4; supplemental experimental procedures). This method afforded monomer mole balances of 100% ± 5% at all levels of partial conversion investigated. We used trimethylsilyl derivatization with GC-MS to identify dimeric compounds at different levels of conversion (Figures 1B and S5; supplemental experimental procedures). Generally, both monomeric and dimeric species followed similar conversion and selectivity trends to those observed during vapor-phase Mo_2C HDO with model compounds.[37,44,58] The first functional groups to undergo deoxygenation are the γ-hydroxyl groups (e.g., PG-OH), generating guaiacol and syringol derivatives. Next, deoxygenation of the methoxy group (e.g., PG) produces phenolics. Finally, phenolics (e.g., propylphenol, PP) are cleaved to produce alkylbenzenes.

Evaluating solvent-free lignin oil stability

Although 2 wt % RCF oil in toluene was a useful system for the development of analytical methods, toluene only dissolves ~70 wt % of the RCF oil, extracting low molecular weight components preferentially (Figures S6 and S7). For this reason, neat RCF oil was used as the feedstock for all subsequent studies. To study the stability of solvent-free RCF oil under elevated temperatures and determine acceptable operating temperatures for the HDO process, we performed catalyst-free flow experiments using conditions otherwise amenable to HDO chemistry (full conditions and protocols in supplemental experimental procedures). Reactor temperatures of 325°C, 350°C, and 375°C showed lignin oil mass recoveries of 98.7 (±1.2), 98.5 (±2.0), and 98.6 (±2.5) wt %, respectively, whereas at 400°C, the mass recovery was 93.2 (±0.9) wt % (Figure 2A; supplemental experimental procedures). PG-OH and PS-OH, which make up 15 wt % of the RCF oil feed, were the most sensitive monomers to

Please cite this article in press as: Stone et al., Continuous hydrodeoxygenation of lignin to jet-range aromatic hydrocarbons, Joule (2022), https://doi.org/10.1016/j.joule.2022.08.005

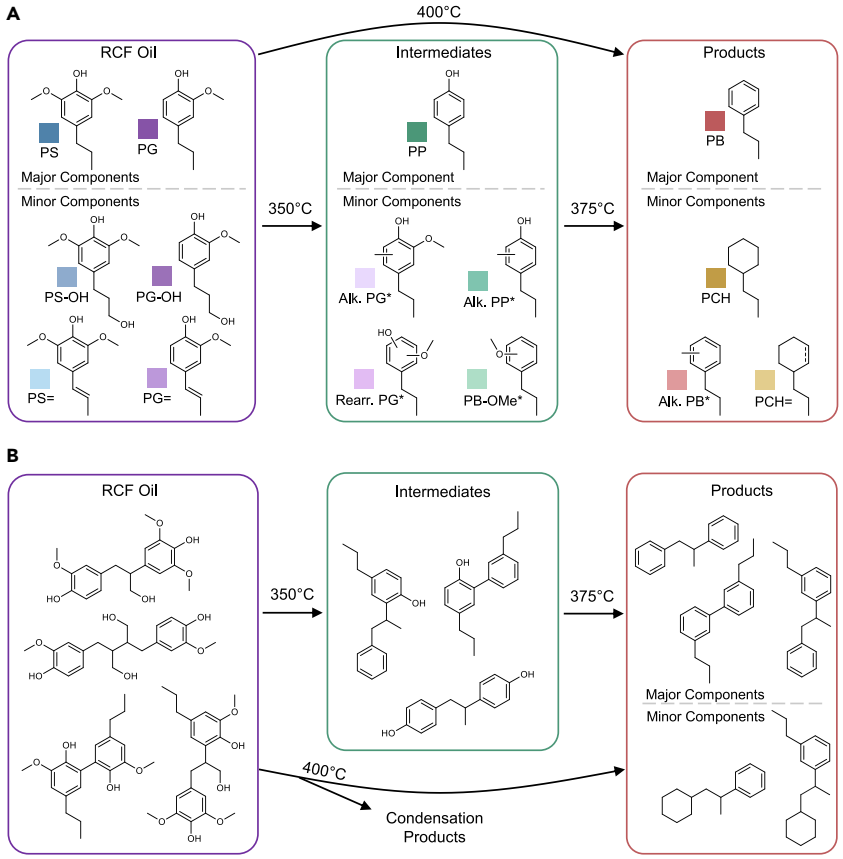

Figure 1. Overview schematic of HDO of RCF lignin oil

(A) Summary of the lignin monomers quantified during this study at all levels of partial conversion, along with the codes and colors used throughout this work. Monomer conversion in single pass or dual pass achieves similar results yielding propylbenzene as a major product. The darker shades of each color represent the major reaction pathway on Mo_2C and the lighter shades are products resulting from side-reactions, including rearrangement of the functional group position and ring alkylation (products noted with an asterisk), which have previously been observed during deoxygenation with molybdenum oxide catalysts.[35,59]

Abbreviations are as follows: PS, propylsyringol; PS, propenylsyringol; PS-OH, dihydrosinapyl alcohol; PG, propylguaiacol; PG, propenylguaiacol; PG-OH, dihydroconiferyl alcohol; PP, propylphenol; Alk. PG, methyl-propylguaiacol; Alk. PP, methyl-propylphenol; Rearr. PG, methoxy-propylphenol; PB-OMe, propylanisole; PB, propylbenzene; PCH, propylcyclohexane.

(B) Examples of dimers identified in the feed, intermediates, and products. Dimer conversion is sensitive to temperature with a parallel pathway toward condensation products at elevated temperatures.

temperature, with combined recoveries of 90.0, 87.9, 40.2, and 17.8 wt % at 325°C, 350°C, 375°C, and 400°C, respectively. Additionally, a combined 5.6 wt % of rearranged, alkylated, and partially deoxygenated monomeric products were formed during the catalyst-free experiment at 400°C. Changes in the molecular weight distribution of the lignin oil, characterized using GPC and GC-MS data of derivatized samples, indicated that increasing the temperature from 325°C to 400°C progressively decreased dimer concentrations and promoted the formation of new oligomers via condensation reactions (Figures 2B and S10).

Mo_2C catalyst activity during HDO of lignin oil

We next evaluated both the activity and stability of the Mo_2C for the continuous HDO of undiluted lignin oil at temperatures below 400°C to reduce deleterious

Please cite this article in press as: Stone et al., Continuous hydrodeoxygenation of lignin to jet-range aromatic hydrocarbons, Joule (2022), https://doi.org/10.1016/j.joule.2022.08.005

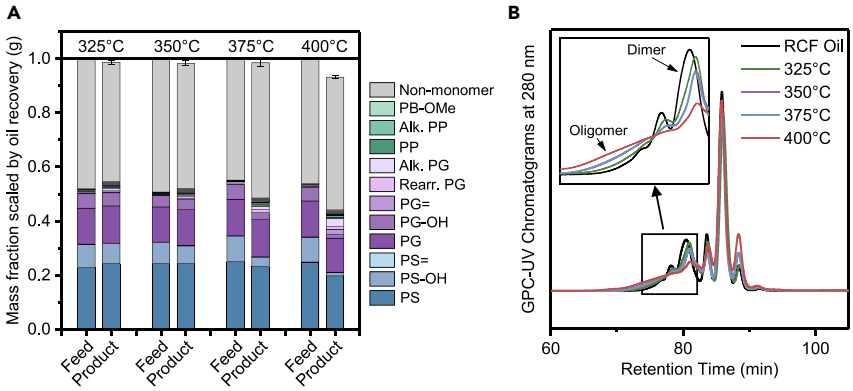

Figure 2. Catalyst-free control experiments to evaluate lignin oil stability

(A) Mass balance on steady-state samples collected during catalyst-free control experiments. The bars show mass fractions of monomers (in color) and non-monomers (in gray), and the product bars are scaled by the overall mass recovery. The height of the bar is the average value, and the error bars show one standard deviation for 3 steady-state samples. The feed bar is included for each experiment to account for slight variability between batches of RCF oil. Tabulated data are included in Table S13.

(B) GPC on the feed ("RCF oil") and the products from catalyst-free control experiments at different temperatures, with the inset showing the dimer and oligomer portion of the curve to highlight the shift in product distribution with increasing temperature. All samples were prepared to the same concentration of 2 mg/mL, and the traces were not normalized or scaled.

lignin condensation (Figure 3). To avoid structural changes caused by the exposure of the carbide phase to molecular oxygen, fresh Mo_2C was synthesized *in situ* via the carburization of ammonium molybdate tetrahydrate (AMT) immediately prior to the start of each experiment (supplemental experimental procedures). At 350°C and a weighted hourly space velocity (WHSV) of 2.35 $g_{lignin}/g_{catalyst}/h$, a steady-state monomer oxygen conversion of 65.8 $\pm$ 0.05 mol % was achieved with major monomeric products of 50.2 mol % PP, 13.8 mol % propylbenzene (PB), and 11.6 mol % propylanisole (PB-OMe) (Figure 3A). Analysis of the vapor-phase effluent during steady-state conversion at 350°C showed major products of CO (29.5% of vapor composition) and CH_4 (18.0%), along with minor products of CO_2 (2.2%), C_2H_6 (1.1%), and C_3H_8 (0.7%) (Figures S11 and S12; Table S5). Following the transient period at the beginning of the reaction resulting from the start-up procedure, the catalyst operated at steady state without deactivation for over 8 h on stream, achieving an estimated turnover number (TON) of 182 based on monomer oxygen atoms removed per active site, a Brunauer-Emmett-Teller (BET) surface area of 25.4 m^2/g, and assumed active site density of 12.74 Mo/nm^2 (Figures S13 and S14; Table S6; supplemental experimental procedures). This TON is a lower-limit estimation, as it only includes the monomers (which can be quantified with a mole balance > 90%) and does not account for the deoxygenation of dimers or larger oligomers. Despite achieving stable deoxygenation at these conditions, neither doubling the residence time (WHSV = 1.175 h^{-1}) nor recycling the partially deoxygenated oil over a fresh catalyst bed at 350°C (Figure S15) resulted in complete monomer deoxygenation. Higher temperatures were required to activate the aryl–OH bonds, with 375°C and a WHSV = 2.35 h^{-1} achieving 48.5% removal of phenolic groups. Figures 3B and 3C show the effect of temperature on catalyst stability. Transient data collected at 300°C and 325°C from 2.5 to 6 h on stream showed steady deactivation profiles with a decrease in monomer oxygen conversion of 58 to 52 mol % for 325°C and 32 to 22 mol % for 300°C. Although temperatures as low as 150°C have been used to deoxygenate anisole[58] and 280°C to achieve near

Please cite this article in press as: Stone et al., Continuous hydrodeoxygenation of lignin to jet-range aromatic hydrocarbons, Joule (2022), https://doi.org/10.1016/j.joule.2022.08.005

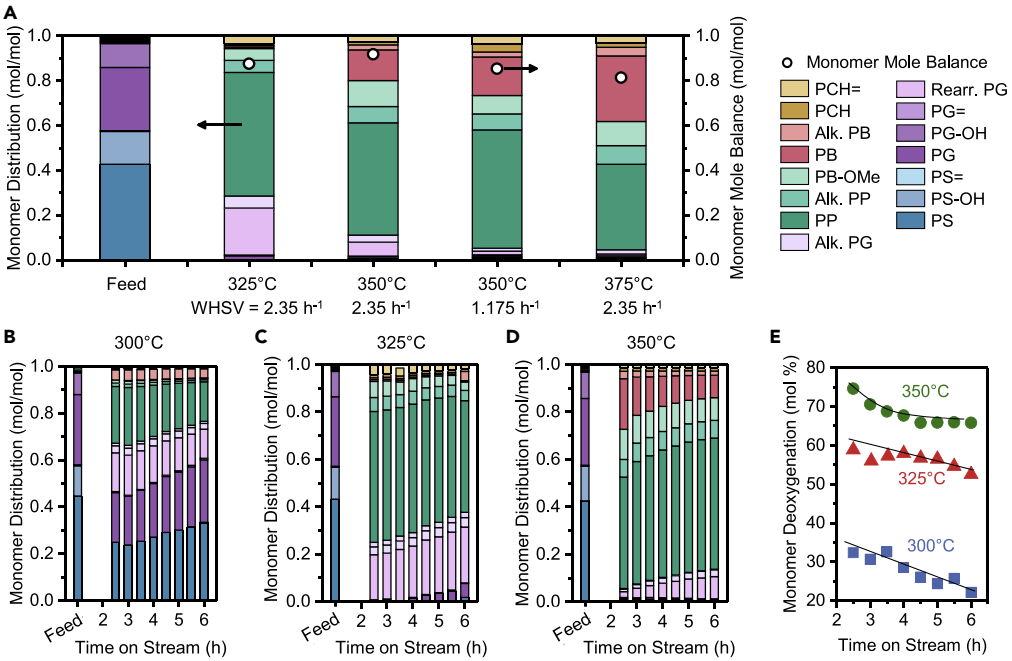

Figure 3. Evaluating activity and stability of Mo_2C for solvent-free lignin HDO

(A) Steady-state results of monomer distribution and monomer mole balance from HDO experiments flowing neat RCF lignin oil ("feed") over a packed bed of 2.88 g Mo_2C (60–100 mesh) in a trickle-bed reactor. Steady-state results were taken after 2.5 h on stream, combined from several hours, and the water formed during reaction was removed prior to performing mass and mole balance calculations (supplemental experimental procedures). Each bar is labeled with the reactor temperature and the weighted hourly space velocity (WHSV) calculated as the mass flowrate of lignin oil divided by mass of catalyst. Data are included in Table S14.

(B–D) The transient distribution of quantified monomers as a function of time on stream at (B) 300°C, (C) 325°C, and (D) 350°C and 0.1 mL/min lignin oil (WHSV = 2.35 h^{-1}).

(E) The conversion of oxygen from the monomer fraction for each experiment shown in (B)–(D), plotted as the mole percent of oxygen removed from the monomers at each time on stream (calculation in supplemental experimental procedures). Transient data for 375°C are included in Figure S27. Constant conditions: 900 psi, 2.88 g Mo_2C (60–100 mesh), 90 mL/min H_2, and toluene at 1 mL/min for 30 min during start-up.

complete deoxygenation of model phenolic mixtures to aromatics at steady state[44] with Mo_2C, our data indicate that temperatures of 350°C and 375°C are needed for stable removal of methoxy and phenolic groups in neat lignin oil, respectively. These results on activity and stability resemble the performance of MoO_3 during HDO.[46,47,59] Although PXRD analysis of the catalyst after reaction does not show bulk oxidation to MoO_3 (Figure S16), *in situ* techniques have shown the surface of Mo_2C is oxidized during reaction with oxygenates.[45,48] Taken together, the trends in our reactivity data indicate that the surface of Mo_2C is likely oxidized by lignin oil to a greater extent than has been observed in previous reports with model compounds,[46,48] thereby necessitating the use of higher temperatures and hydrogen pressures to maintain HDO activity. This potentially explains why prior work on HDO of oxygen-rich real lignin feeds with Mo_2C did not achieve complete deoxygenation[49–51] and highlights the difficulty in translating the results of model systems to biomass feedstocks.

Achieving deep deoxygenation to aromatic hydrocarbons

Together, lignin oil stability (Figure 2) and catalyst activity (Figure 3) experiments revealed an important trade-off in lignin oil HDO: low temperatures result in catalyst deactivation but achieve high carbon balances by preserving oligomers, whereas high temperatures are necessary to maintain catalyst activity and achieve full deoxygenation but result in the loss of dimers through condensation. We evaluated

Please cite this article in press as: Stone et al., Continuous hydrodeoxygenation of lignin to jet-range aromatic hydrocarbons, Joule (2022), https://doi.org/10.1016/j.joule.2022.08.005

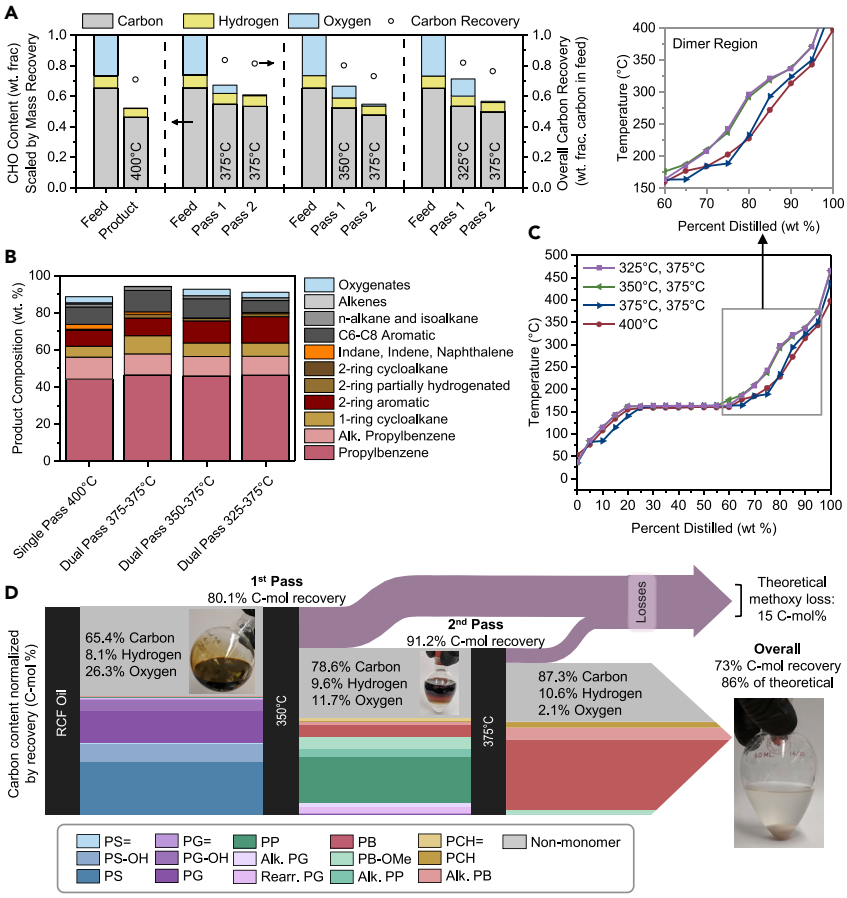

Figure 4. Optimizing deep deoxygenation of lignin oil for jet-range aromatic production

(A) Carbon, oxygen, and hydrogen content in the oil on a mass basis, as determined via total carbon analysis. The weight percent results of total carbon analysis were multiplied by the mass recovery of oil at steady state after removing the aqueous fraction to generate the plot. The data are provided in Table S9.

(B) Results of quantitative GC × GC analysis of the final deoxygenated oils from each of the experiments shown in (A). The data are provided in Table S7.

(C) Simulated distillation generated by the ASTM D2887 method of the deoxygenated product from each multi-pass experiment, with a zoomed-in plot on the dimer region. Protocols and conditions are in supplemental experimental procedures.

(D) Production of deoxygenated lignin oil using optimized multi-pass conditions. The Sankey diagram shows the carbon balance on each pass of the optimum multi-pass experiment. The carbon content in the whole oil was determined using total carbon analysis. The monomer carbon content was determined with GC-FID analysis and is plotted as a fraction of the total carbon content. The carbon content was multiplied by the steady-state recovery of the oil (by mass) across each pass. Photos show the oil at each stage of the process, with water (bottom phase) formed during the reaction separating from the deoxygenated organics (top phase). The data are provided in Table S15. Conditions: 2.88 g Mo_2C (60–100 mesh), 0.1 mL/min lignin oil, 90 mL/min H_2, 900 psi, 350°C first pass, 375°C second pass, and toluene at 1 mL/min for 30 min during start-up.

two routes for generating deeply deoxygenated oil products: (1) increasing the temperature and the residence time in a single pass at 400°C and WHSV = 1.175 h^{-1} and (2) operating in a two-pass mode wherein an initial HDO run is performed at an intermediate temperature to generate a mixture of partially deoxygenated monomers and oligomers that is more resistant toward subsequent condensation reactions, followed by a second pass at a higher temperature to achieve full deoxygenation. For the two-pass experiments, first-pass products were collected at 325°C, 350°C, or 375°C, each over a fresh catalyst bed. Next, these products were deoxygenated at

Please cite this article in press as: Stone et al., Continuous hydrodeoxygenation of lignin to jet-range aromatic hydrocarbons, Joule (2022), https://doi.org/10.1016/j.joule.2022.08.005

375°C in a second run with a fresh catalyst bed. Figure 4A summarizes the carbon, hydrogen, and oxygen content of each oil scaled by the mass recovery from each pass along with the overall carbon recovery. After the first pass at 400°C, 375°C, 350°C, and 325°C, 0.7, 8.0, 11.7, and 15.8 wt % oxygen remained, respectively. This was reduced to 1.0, 2.1, and 1.2 wt % for 375–375°C, 350–375°C, and 325–375°C, respectively. The near complete deoxygenation of the products was confirmed with HSQC NMR (Figure S17) and derivatization + GC-MS (Figure S18). The final monomer product distributions were similar in all cases, with propylbenzene selectivity values of ca. 78 mol %. The dimer products were more sensitive to temperature, showing 8.9, 9.5, 11.9, and 14.2 wt % dimer content for first pass temperatures of 400°C, 375°C, 350°C, and 325°C, respectively, as determined by quantitative GC × GC analysis (Figures 4B and S19–S22; Table S7; supplemental experimental procedures). This trend in dimer recovery was supported by simulated distillation (Figure 4C) and additional chromatography techniques (Figures S23 and S24; Table S8).

Two-pass operation with 350°C followed by 375°C achieved an optimal balance for catalyst stability and jet-range aromatic production. Indeed, 350°C was the optimal temperature to maintain stable catalyst activity at partial deoxygenation in the first pass (total product oxygen content of 11.7%), whereas higher temperatures of 375°C and 400°C resulted in an elevated loss of aromatic dimers. Figure 4D summarizes the optimal overall process, where we obtained a reduction in total oxygen content from 26.3 to 2.1 mol % (95.7% conversion). Additionally, nitrogen content decreased during reaction from 0.19 mol % in RCF oil to 0.13 mol % after the first pass at 350°C and 0.028 mol % after the second pass at 375°C. These conditions achieved an unprecedented 73.1 C-mol % recovery (86% of theoretical based on removal of methoxy groups, balanced equation in Figure S25) and 87.5% monomer selectivity toward aromatic hydrocarbons. For reference, recent reports have shown yields between 10–30 and 30–50 wt % via one- and two-step processes, respectively, whereas our process's mass recovery is consistently between 50 and 60 wt % (Table S9) while achieving higher levels of deoxygenation than those studies discussed.[60] Photos of samples taken directly from the reactor are included in Figure 4D, demonstrating the natural phase separation of the water formed during reaction (bottom phase) and the clear hydrocarbon solution (top phase) obtained after the second pass. Analysis of the post-reaction aqueous phase showed 1.2% carbon content in the water, along with trace leached molybdenum species (Tables S10 and S11). GC × GC quantification of the organic phase determined a final aromatic dimer (C14-C20) content of 11.9 wt % and aromatic monomer (C9-C12) content of 56 wt %, summing to 67.9 wt % of jet-range aromatics in the final oil.

Tier α characterization of the deoxygenated hydrocarbon product

Tier α testing was conducted on the deoxygenated products from the 350–375°C dual pass HDO process and used to make initial property predictions (Figure 5).[61,62] The composition and properties reported in Figure 5 represent a likely finished product composition and distribution. Specifically, higher and lower molecular weight compounds, as well as oxygenates (2.87 wt % in the original material), were removed for the following analysis. Collectively, 64.23 wt % of the HDO process material is represented in Figure 5A. The hydrocarbon type analysis (Table S12) used for property predictions and the compositional information (Data S1) for the original material are reported in the supplemental information. Figure 5A compares the distribution of products in the deoxygenated oil (purple to yellow color map) compared with an average conventional Jet A (POSF 10325, shaded green). These data were generated using jet fuel-specific GC × GC chromatography methods reported elsewhere and used for 93 other samples.[63] Vacuum ultra violet

Please cite this article in press as: Stone et al., Continuous hydrodeoxygenation of lignin to jet-range aromatic hydrocarbons, Joule (2022), https://doi.org/10.1016/j.joule.2022.08.005

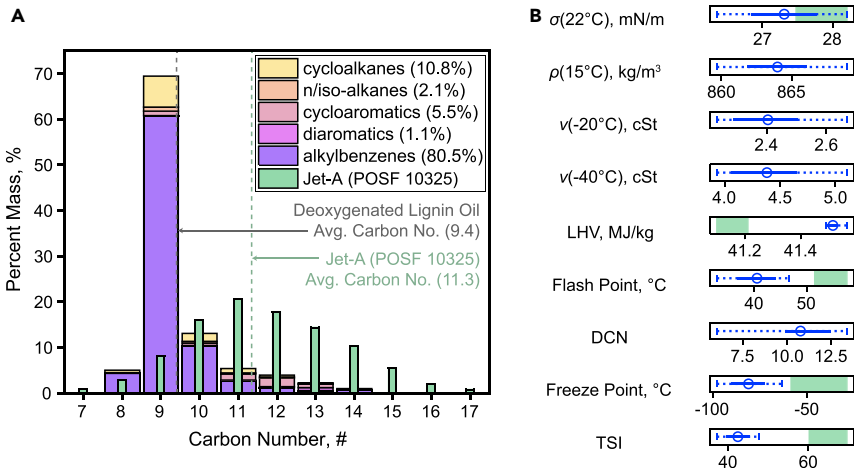

Figure 5. Tier α testing of deoxygenated lignin oil

(A) Distribution of the final product composition of deoxygenated lignin oil arranged by species type and carbon number (stacked bars with purple to yellow color map). This represents 64.2 wt % of the deoxygenated product from the 350°C–375°C dual pass condition (summarized in Figure 4D) after removing residual oxygenates and higher and lower molecular weight species. An average jet fuel carbon number distribution is included for reference (green bars). Vertical dashed lines show the average carbon numbers of the deoxygenated lignin oil sample (gray) and Jet A (green).

(B) Property predictions of the lignin-derived aromatic blendstock compared with a range of conventional fuel aromatics (green shaded region). Solid lines correspond to the 68% confidence interval and capped dashed lines are for the 95% CI. σ, surface tension; ρ, density; ν, viscosity; LHV, lower heating value; DCN, derived cetane number; TSI, threshold sooting index.

(VUV) spectroscopy identified 23 specific isomers, which accounted for 77 wt % of the predictive sample. Approximately 60 wt % of the material reported in Figure 5A is composed of *n*-propylbenzene. Figure 5B illustrates the predicted (open circles) critical operability properties for the distilled cut. The solid lines are the 68% confidence interval (CI), and the capped dashed lines are the 95% CI for each prediction. The predicted property range of aromatics in conventional fuels is shown in shaded green. Overall, properties are near or more favorable than conventional fuel aromatics. Specifically, the surface tension (σ), freeze point, and threshold sooting index (TSI) are predicted to be lower than conventional fuel aromatics, whereas the lower heating value (LHV) is predicted to be higher for the deoxygenated lignin oil compared with conventional fuel aromatics. The viscosity (ν) for the deoxygenated lignin oil composition is predicted to be lower than the ASTM maximum for aviation fuel at −20°C (8 cSt) and −40°C (12 cSt), and despite the lower average carbon number of the deoxygenated lignin oil (9.4) compared with Jet A (11.3), the lignin oil flash point is predicted to be above the minimum flash point of Jet A (38°C).

DISCUSSION

This work demonstrates that lignin stability is a key constraint under typical HDO conditions. Our data indicate that the loss of dimers at higher operating temperatures (>350°C) is likely occurring via condensation reactions upstream of the catalyst bed. The catalyst-free control experiments show a trend in which increasing temperature results in the loss of dimers and formation of a larger oligomer tail on the GPC chromatograms of each product. Similar trends are observed in HDO experiments with Mo_2C present, where the dimer content of the deeply deoxygenated products decreases with increasing first-pass temperature. This indicates the same dimer-loss mechanism occurs whether or not catalyst is present in the system. Although this work does not seek to elucidate the fundamental mechanism of lignin condensation in our system,

Please cite this article in press as: Stone et al., Continuous hydrodeoxygenation of lignin to jet-range aromatic hydrocarbons, Joule (2022), https://doi.org/10.1016/j.joule.2022.08.005

there is substantial precedent for the propensity of lignin species to condense under harsh conditions.[14,64–66] We note, however, that coking is an unlikely mechanism for carbon loss since the catalyst did not appear to deactivate at higher temperatures where dimer loss is more significant and the quartz chips upstream of the catalyst contained minimal residual carbon post reaction (Figure S26). Furthermore, the monomeric fraction of deeply deoxygenated oil is nearly identical, regardless of first pass temperature, and only small quantities (2%–3%) of C2-C3 hydrocarbons are detected in the vapor phase during reaction (Figure S11), indicating that hydrocracking pathways for dimer degradation are unlikely. Ultimately, this work presents a reaction engineering solution to lignin instability using two-pass HDO, with the first pass used for stabilization via partial conversion and the second pass for deep deoxygenation. We anticipate that this strategy for lignin upgrading with high atom economy could be broadly applicable to other lignin feedstocks.

HDO reactions with Mo_2C selectively cleaved C–O bonds while leaving the C–C structure of the lignin substrate intact. In addition to minimizing the consumption of hydrogen, this selectivity indicates that the distribution of HDO products could be tuned by modifying the lignin feedstock itself. For example, a lignin substrate with a higher fraction of dimeric components could be utilized to increase the C14-C20 aromatic fraction in the resulting deoxygenated product. Furthermore, the carbon backbone of the dimer and oligomer fraction retains sufficient chemical functionality during reaction to differentiate between types of lignin inter-unit linkages that are present *in planta* (e.g., β-5 versus 5-5). The alkylation and rearrangement reactions observed were restricted to methylation of the aromatic rings and rearrangement of the positions of the oxygen functional groups on the ring, allowing us to distinguish the carbon backbone of 5-5, β-β, and (β-1, β-5) dimers, recognizing that the lattermost two dimers could be scrambled by alkylation reactions. Quantification of highly oxygenated and diverse lignin dimers and oligomers obtained from hydrogenolysis remains a significant challenge at the forefront of lignin analytics.[19,55–57] Conversely, quantification of deoxygenated aromatic dimers is readily available using 2D GC × GC techniques developed for hydrocarbon analytics.[63] Additional optimization will be necessary to minimize dimer condensation by further stabilizing the feed or reducing the HDO operating temperatures. However, this work provides preliminary evidence that direct deoxygenation of lignin oil with Mo_2C could provide an analytical opportunity to quantitatively backtrack lignin C–C bond distributions *in planta*.

This work also motivates the development of catalysts that can achieve stable HDO of real lignin feedstocks at low temperatures. Notably, the behavior of the catalyst under reaction with neat lignin oil was distinctly different than vapor-phase model compound studies reported to date. Furthermore, although the existing literature contains a strong fundamental framework from which to understand the impact of controlled Mo_2C surface oxidation on model compound reactivity, the parameters that determine extent of catalyst oxidation under reaction conditions with real lignin feeds have not been mapped and are not well understood. Understanding the factors that drive catalyst surface deactivation under reaction conditions with real feedstocks could enable rational catalyst design or reaction engineering solutions to mitigate catalyst deactivation and enable lower operating temperatures. Altogether, performing experiments in a trickle-bed reactor to generate continuous, steady-state HDO data using a real lignin feedstock, along with rigorous analytics to track carbon balances and individual components, was essential to understanding the limitations of this complex system.

Tier α characterization showed that ~64% of the deoxygenated aromatics resulting from this process fall within a suitable range for use in SAFs. Modeled properties

Please cite this article in press as: Stone et al., Continuous hydrodeoxygenation of lignin to jet-range aromatic hydrocarbons, Joule (2022), https://doi.org/10.1016/j.joule.2022.08.005

produced encouraging results as many of them were predicted to be performance-advantaged relative to conventional fuel aromatics, including LHV, freeze point, and surface tension. Most importantly, the lower molecular weight aromatic hydrocarbons found in the sample are desirable in aviation turbine fuel.[67] Aromatics are needed for the fuel to be drop-in and fungible with existing aircrafts and infrastructure. Specifically, aromatics are required to achieve proper material compatibility and a dielectric constant similar to that in conventional fuel.[13,67] However, aromatics are also associated with increased sooting to form non-volatile particulate matter emissions, which are carcinogenic and may impact the formation of contrails.[68] The latter could be even more important than CO_2 emissions for the radiative forcing impact of aviation.[69] Lower molecular weight aromatics, as reported here, are associated with lower sooting potentials (TSI in Figure 5B) compared with higher molecular weight aromatics. Additionally, the lignin oil sample studied here has many similar compositional properties to a previously studied synthetic aromatic kerosene, which is currently undergoing the ASTM International qualification process.[67] The similarity to the other SAF pathway could thus aid the qualification process of this route. Finally, some existing biorefinery models to produce SAF do not leverage lignin and produce SAFs absent of aromatic content.[11] The combination of this lignin route with other routes, which are non-competitive with lignin as a feedstock and do not produce aromatics, could ultimately produce a 100% SAF composition.

Further development and analysis will be necessary to evaluate the complete viability of the lignin HDO process for commercial SAF production. The 350°C–375°C dual pass condition, which was optimized for catalyst stability and dimer recovery, yielded an oil which contained 2% oxygen, a level that is still too high for direct use in jet fuel.[10] However, we achieved deeper deoxygenation at higher operating temperatures (0.7% O remaining after 400°C), and there was some variability between runs, with the 325–375°C experiment yielding only 1.2% O remaining. Distillation and blending, which would be required to use our deoxygenated oil with no additional chemical processing, would also inherently reduce the oxygen content. Regardless, future optimization and process modeling that aims at assessing fuel/process viability would need to include residual oxygen content as a key constraint. Future work will involve the development and optimization of hydrogenation, ring-opening, and/or hydrocracking reactions, which could be implemented to convert a fraction of the lignin-derived aromatics to other paraffinic compounds (including cycloalkanes and *iso*/*n*-alkanes), thereby generating an entirely lignin-derived SAF. As noted in the introduction, other catalysts have demonstrated the production of alkanes directly from lignin, primarily via a metal catalyzed ring hydrogenation followed by acid catalyzed dehydration.[26–34] Our process is unique in the high atom economy achieved via direct deoxygenation to aromatics, which affords more options in subsequent hydrotreating or blending of fractions of the aromatic product. Finally, ongoing techno-economic analyses and life cycle assessments are geared toward identifying critical areas for further development and integration of our product into a 100% SAF blend.

EXPERIMENTAL PROCEDURES

Resource availability

Lead contact

Further information and requests for resources should be directed to and will be fulfilled by the lead contact, Yuriy Román-Leshkov (Y.R.-L.) (yroman@mit.edu).

Materials availability

Materials are available upon request. There are restrictions to the availability of oils generated in this study due to limited lab production capacity.

Data and code availability

The datasets in this article are provided in the supplemental information.

SUPPLEMENTAL INFORMATION

Supplemental information can be found online at https://doi.org/10.1016/j.joule.2022.08.005.

ACKNOWLEDGMENTS

We thank Amber Phillips for contributions to figure design and Joel Miscall for assistance with trace metals analysis. We also thank Karthick Murugappan for contributions to the inception of this research direction. This work was authored in part by Alliance for Sustainable Energy, LLC, the manager and operator of the National Renewable Energy Laboratory for the U.S. Department of Energy (DOE) under contract no. DE-AC36-08GO28308. The work was initially funded by The Center for Bioenergy Innovation, a U.S. Department of Energy Research Center supported by the Office of Biological and Environmental Research in the DOE Office of Science. G.T.B., J.S.H, and Y.R.-L. acknowledge funding from the US Department of Energy Bioenergy Technologies Office. Y.R.-L. and W.P.M. acknowledge funding from by Eni S.p.A. through the MIT Energy Initiative. The views expressed in the article do not necessarily represent the views of the DOE or the U.S. Government.

AUTHOR CONTRIBUTIONS

Conceptualization, M.L.S., Y.R.-L., W.P.M., M.S.W., E.M.A., and G.T.B.; methodology, M.L.S., E.M.A., W.P.M., and M.S.W.; investigation, M.L.S., M.S.W., W.P.M., D.C.B., E.C., A.R.C.M., and Y.L.; supervision, Y.R.-L., G.T.B., and J.S.H.; funding acquisition, Y.R.-L. and G.T.B.; visualization, M.L.S., M.S.W., and D.C.B.; writing – original draft, M.L.S. and M.S.W.; writing – review & editing, Y.R.-L., G.T.B., J.S.H., D.C.B., W.P.M., E.C., A.R.C.M., Y.L., and E.M.A.

DECLARATION OF INTERESTS

M.L.S., M.S.W., G.T.B., and Y.R.-L. are inventors on a patent application that covers the HDO chemistry to deoxygenate lignin components.

Received: June 9, 2022
Revised: June 27, 2022
Accepted: August 15, 2022
Published: September 22, 2022

REFERENCES

1. U.S. Energy Information Administration (2020). Annual energy outlook 2020. (Office of Energy Analysis, United States Department of Energy). https://www.eia.gov/outlooks/aeo/.

2. International Air Transport Association (2021). Net-zero carbon emissions by 2050. https://www.iata.org/en/pressroom/2021-releases/2021-10-04-03/.

3. Karatzos, S., van Dyk, J.S., McMillan, J.D., and Saddler, J. (2017). Drop-in biofuel production via conventional (lipid/fatty acid) and advanced (biomass) routes. Part I. Biofuel Bioprod. Biorefin *11*, 344–362. https://doi.org/10.1002/bbb.1746.

4. Goh, B.H.H., Chong, C.T., Ge, Y., Ong, H.C., Ng, J.-H., Tian, B., Ashokkumar, V., Lim, S., Seljak, T., and Józsa, V. (2020). Progress in utilisation of waste cooking oil for sustainable biodiesel and biojet fuel production. Energy Convers. Manag. *223*, 113296. https://doi.org/10.1016/j.enconman.2020.113296.

5. O'Malley, J., Pavlenko, N., and Searle, S. (2021). Estimating sustainable aviation fuel feedstock availability to meet growing European Union demand. (International Council on Clean Transportation). https://theicct.org/publication/estimating-sustainable-aviation-fuel-feedstock-availability-to-meet-growing-european-union-demand/.

6. Hadaller, O.J., and Johnson, J.M. (2006). World fuel sampling program. Coordinating Research Council Report No. 647. https://crcao.org/crc-report-no-647/.

7. Edwards, J.T. (2017). Reference jet fuels for combustion testing. 55th AIAA Aerospace Sciences Meeting. https://www.caafi.org/news/pdf/Edwards_AIAA-2017-0146_Reference_Jet_Fuels.pdf.

8. Hileman, J.I., and Stratton, R.W. (2014). Alternative jet fuel feasibility. Transp. Policy *34*, 52–62. https://doi.org/10.1016/j.tranpol.2014.02.018.

9. Cheng, F., and Brewer, C.E. (2017). Producing jet fuel from biomass lignin: potential pathways to alkyl-benzenes and cycloalkanes. Renew. Sustain. Energ. Rev. *72*, 673–722. https://doi.org/10.1016/j.rser.2017.01.030.

10. ASTM International (2014). Standard specification for aviation turbine fuels

containing synthesized hydrocarbons. (ASTM International). https://www.astm.org/d7566-14.html.

11. Holladay, J., Abdullah, Z., and Heyne, J. (2020). Sustainable aviation fuel: review of technical pathways. (Office of Energy Efficiency & Renewable Energy). https://www.energy.gov/eere/bioenergy/downloads/sustainable-aviation-fuel-review-technical-pathways-report.

12. Beck, T., Blank, B., Jones, C., Woods, E., and Cortright, R. (2016). Production of aromatics from di- and polyoxygenates. US patent WO2014152370A2.

13. Kramer, S., Andac, G., Heyne, J., Ellsworth, J., Herzig, P., and Lewis, K.C. (2022). Perspectives on fully synthesized sustainable aviation fuels: direction and opportunities. Front. Energy Res. *9*, 782823. https://doi.org/10.3389/fenrg.2021.782823.

14. Schutyser, W., Renders, T., Van den Bosch, S., Koelewijn, S.F., Beckham, G.T., and Sels, B.F. (2018). Chemicals from lignin: an interplay of lignocellulose fractionation, depolymerisation, and upgrading. Chem. Soc. Rev. *47*, 852–908. https://doi.org/10.1039/c7cs00566k.

15. Langholtz, M.H., Stokes, B.J., and Eaton, L.M. (2016). 2016 billion-ton report: advancing domestic resources for a thriving bioeconomy. (U.S. Department of Energy). https://www.osti.gov/biblio/1435342-billion-ton-report-advancing-domestic-resources-thriving-bioeconomy-volume-economic-availability-feedstocks.

16. Zakzeski, J., Bruijnincx, P.C.A., Jongerius, A.L., and Weckhuysen, B.M. (2010). The catalytic valorization of lignin for the production of renewable chemicals. Chem. Rev. *110*, 3552–3599. https://doi.org/10.1021/cr900354u.

17. Abu-Omar, M.M., Barta, K., Beckham, G.T., Luterbacher, J.S., Ralph, J., Rinaldi, R., Román-Leshkov, Y., Samec, J.S.M., Sels, B.F., and Wang, F. (2021). Guidelines for performing lignin-first biorefining. Energy Environ. Sci. *14*, 262–292. https://doi.org/10.1039/D0EE02870C.

18. Anderson, E.M., Stone, M.L., Katahira, R., Reed, M., Beckham, G.T., and Román-Leshkov, Y. (2017). Flowthrough reductive catalytic fractionation of biomass. Joule *1*, 613–622. https://doi.org/10.1016/j.joule.2017.10.004.

19. Van den Bosch, S., Schutyser, W., Vanholme, R., Driessen, T., Koelewijn, S.-F., Renders, T., De Meester, B., Huijgen, W.J.J., Dehaen, W., Courtin, C.M., et al. (2015). Reductive lignocellulose fractionation into soluble lignin-derived phenolic monomers and dimers and processable carbohydrate pulps. Energy Environ. Sci. *8*, 1748–1763. https://doi.org/10.1039/C5EE00204D.

20. Anderson, E.M., Stone, M.L., Hülsey, M.J., Beckham, G.T., and Román-Leshkov, Y. (2018). Kinetic studies of lignin solvolysis and reduction by reductive catalytic fractionation decoupled in flow-through reactors. ACS Sustainable Chem. Eng. *6*, 7951–7959. https://doi.org/10.1021/acssuschemeng.8b01256.

21. Questell-Santiago, Y.M., Galkin, M.V., Barta, K., and Luterbacher, J.S. (2020). Stabilization strategies in biomass depolymerization using chemical functionalization. Nat. Rev. Chem. *4*, 311–330. https://doi.org/10.1038/s41570-020-0187-y.

22. Shuai, L., Amiri, M.T., Questell-Santiago, Y.M., Héroguel, F., Li, Y., Kim, H., Meilan, R., Chapple, C., Ralph, J., and Luterbacher, J.S. (2016). Formaldehyde stabilization facilitates lignin monomer production during biomass depolymerization. Science *354*, 329–333. https://doi.org/10.1126/science.aaf7810.

23. Lan, W., Amiri, M.T., Hunston, C.M., and Luterbacher, J.S. (2018). Protection group effects during α, γ-diol lignin stabilization promote high-selectivity monomer production. Angew. Chem. Int. Ed. Engl. *130*, 1370–1374. https://doi.org/10.1002/anie.201710838.

24. Brandner, D.G., Kruger, J.S., Thornburg, N.E., Facas, G.G., Kenny, J.K., Dreiling, R.J., Morais, A.R.C., Renders, T., Cleveland, N.S., Happs, R.M., et al. (2021). Flow-through solvolysis enables production of native-like lignin from biomass. Green Chem *23*, 5437–5441. https://doi.org/10.1039/D1GC01591E.

25. Speight, J.G. (2012). Refining shale oil. In Shale Oil Production Processes, J.G. Speight, ed. (Gulf Professional Publishing), pp. 139–163.

26. Wang, L., Zhang, J., Yi, X., Zheng, A., Deng, F., Chen, C., Ji, Y., Liu, F., Meng, X., and Xiao, F.-S. (2015). Mesoporous ZSM-5 zeolite-supported Ru nanoparticles as highly efficient catalysts for upgrading phenolic biomolecules. ACS Catal *5*, 2727–2734. https://doi.org/10.1021/acscatal.5b00083.

27. Güvenatam, B., Kurşun, O., Heeres, E.H.J., Pidko, E.A., and Hensen, E.J.M. (2014). Hydrodeoxygenation of mono- and dimeric lignin model compounds on noble metal catalysts. Catal. Today *233*, 83–91. https://doi.org/10.1016/j.cattod.2013.12.011.

28. Luska, K.L., Migowski, P., El Sayed, S., and Leitner, W. (2015). Synergistic interaction within bifunctional ruthenium nanoparticle/SILP catalysts for the selective hydrodeoxygenation of phenols. Angew. Chem. Int. Ed. Engl. *54*, 15750–15755. https://doi.org/10.1002/anie.201508513.

29. Schutyser, W., Van den Bossche, G., Raaffels, A., Van den Bosch, S., Koelewijn, S.-F., Renders, T., and Sels, B.F. (2016). Selective conversion of lignin-derivable 4-alkylguaiacols to 4-alkylcyclohexanols over noble and non-noble-metal catalysts. ACS Sustainable Chem. Eng. *4*, 5336–5346. https://doi.org/10.1021/acssuschemeng.6b01580.

30. Mochizuki, T., Chen, S.-Y., Toba, M., and Yoshimura, Y. (2014). Deoxygenation of guaiacol and woody tar over reduced catalysts. Appl. Catal. B *146*, 237–243. https://doi.org/10.1016/j.apcatb.2013.05.040.

31. Mortensen, P.M., Grunwaldt, J.-D., Jensen, P.A., and Jensen, A.D. (2016). Influence on nickel particle size on the hydrodeoxygenation of phenol over Ni/SiO_2. Catal. Today *259*, 277–284. https://doi.org/10.1016/j.cattod.2015.08.022.

32. Dongil, A.B., Ghampson, I.T., García, R., Fierro, J.L.G., and Escalona, N. (2016). Hydrodeoxygenation of guaiacol over Ni/carbon catalysts: effect of the support and Ni loading. RSC Adv *6*, 2611–2623. https://doi.org/10.1039/C5RA22540J.

33. Liu, X., Xu, L., Xu, G., Jia, W., Ma, Y., and Zhang, Y. (2016). Selective hydrodeoxygenation of lignin-derived phenols to cyclohexanols or cyclohexanes over magnetic CoNx@NC catalysts under mild conditions. ACS Catal *6*, 7611–7620. https://doi.org/10.1021/acscatal.6b01785.

34. Zhao, C., He, J., Lemonidou, A.A., Li, X., and Lercher, J.A. (2011). Aqueous-phase hydrodeoxygenation of bio-derived phenols to cycloalkanes. J. Catal. *280*, 8–16. https://doi.org/10.1016/j.jcat.2011.02.001.

35. Anderson, E., Crisci, A., Murugappan, K., and Román-Leshkov, Y. (2017). Bifunctional molybdenum polyoxometalates for the combined hydrodeoxygenation and alkylation of lignin-derived model phenolics. ChemSusChem *10*, 2226–2234. https://doi.org/10.1002/cssc.201700297.

36. Prasomsri, T., Nimmanwudipong, T., and Román-Leshkov, Y. (2013). Effective hydrodeoxygenation of biomass-derived oxygenates into unsaturated hydrocarbons by MoO_3 using low H_2 pressures. Energy Environ. Sci. *6*, 1732–1738. https://doi.org/10.1039/C3EE24360E.

37. Sullivan, M.M., Chen, C.-J., and Bhan, A. (2016). Catalytic deoxygenation on transition metal carbide catalysts. Catal. Sci. Technol. *6*, 602–616. https://doi.org/10.1039/C5CY01665G.

38. Wu, S.-K., Lai, P.-C., Lin, Y.-C., Wan, H.-P., Lee, H.-T., and Chang, Y.-H. (2013). Atmospheric hydrodeoxygenation of guaiacol over alumina-, zirconia-, and silica-supported nickel phosphide catalysts. ACS Sustainable Chem. Eng. *1*, 349–358. https://doi.org/10.1021/sc300157d.

39. Sun, J., Karim, A.M., Zhang, H., Kovarik, L., Li, X.S., Hensley, A.J., McEwen, J.-S., and Wang, Y. (2013). Carbon-supported bimetallic Pd–Fe catalysts for vapor-phase hydrodeoxygenation of guaiacol. J. Catal. *306*, 47–57. https://doi.org/10.1016/j.jcat.2013.05.020.

40. Rensel, D.J., Rouvimov, S., Gin, M.E., and Hicks, J.C. (2013). Highly selective bimetallic FeMoP catalyst for C–O bond cleavage of aryl ethers. J. Catal. *305*, 256–263. https://doi.org/10.1016/j.jcat.2013.05.026.

41. Barrios, A.M., Teles, C.A., de Souza, P.M., Rabelo-Neto, R.C., Jacobs, G., Davis, B.H., Borges, L.E.P., and Noronha, F.B. (2018). Hydrodeoxygenation of phenol over niobia supported Pd catalyst. Catal. Today *302*, 115–124. https://doi.org/10.1016/j.cattod.2017.03.034.

42. Newman, C., Zhou, X., Goundie, B., Ghampson, I.T., Pollock, R.A., Ross, Z., Wheeler, M.C., Meulenberg, R.W., Austin, R.N., and Frederick, B.G. (2014). Effects of support identity and metal dispersion in supported ruthenium hydrodeoxygenation catalysts. Appl. Catal. A *477*, 64–74. https://doi.org/10.1016/j.apcata.2014.02.030.

43. Do, P.T.M., Foster, A.J., Chen, J., and Lobo, R.F. (2012). Bimetallic effects in the hydrodeoxygenation of meta-cresol on γ-Al_2O_3 supported Pt–Ni and Pt–Co catalysts.

Green Chem *14*, 1388–1397. https://doi.org/10.1039/C2GC16544A.

44. Chen, C.-J., Lee, W.-S., and Bhan, A. (2016). Mo_2C catalyzed vapor phase hydrodeoxygenation of lignin-derived phenolic compound mixtures to aromatics under ambient pressure. Appl. Catal. A *510*, 42–48. https://doi.org/10.1016/j.apcata.2015.10.043.

45. Lee, W.-S., Kumar, A., Wang, Z., and Bhan, A. (2015). Chemical titration and transient kinetic studies of site requirements in Mo_2C-catalyzed vapor phase anisole hydrodeoxygenation. ACS Catal *5*, 4104–4114. https://doi.org/10.1021/acscatal.5b00713.

46. Chen, C.-J., and Bhan, A. (2017). Mo_2C modification by CO_2, H_2O, and O_2: effects of oxygen content and oxygen source on rates and selectivity of m-cresol hydrodeoxygenation. ACS Catal *7*, 1113–1122. https://doi.org/10.1021/acscatal.6b02762.

47. Kumar, A., and Bhan, A. (2019). Oxygen content as a variable to control product selectivity in hydrodeoxygenation reactions on molybdenum carbide catalysts. Chem. Eng. Sci. *197*, 371–378. https://doi.org/10.1016/j.ces.2018.12.027.

48. Murugappan, K., Anderson, E.M., Teschner, D., Jones, T.E., Skorupska, K., and Román-Leshkov, Y. (2018). Operando NAP-XPS unveils differences in MoO_3 and Mo_2C during hydrodeoxygenation. Nat. Catal. *1*, 960–967. https://doi.org/10.1038/s41929-018-0171-9.

49. Cattelan, L., Yuen, A.K.L., Lui, M.Y., Masters, A.F., Selva, M., Perosa, A., and Maschmeyer, T. (2017). Renewable aromatics from kraft lignin with molybdenum-based catalysts. ChemCatChem *9*, 2717–2726. https://doi.org/10.1002/cctc.201700374.

50. Jongerius, A.L., Bruijnincx, P.C.A., and Weckhuysen, B.M. (2013). Liquid-phase reforming and hydrodeoxygenation as a two-step route to aromatics from lignin. Green Chem *15*, 3049–3056. https://doi.org/10.1039/C3GC41150H.

51. Grilc, M., Veryasov, G., Likozar, B., Jesih, A., and Levec, J. (2015). Hydrodeoxygenation of solvolysed lignocellulosic biomass by unsupported MoS_2, MoO_2, Mo_2C and WS_2 catalysts. Appl. Cat. B *163*, 467–477. https://doi.org/10.1016/j.apcatb.2014.08.032.

52. Shu, R., Li, R., Lin, B., Wang, C., Cheng, Z., and Chen, Y. (2020). A review on the catalytic hydrodeoxygenation of lignin-derived phenolic compounds and the conversion of raw lignin to hydrocarbon liquid fuels. Biomass Bioenergy *132*, 105432. https://doi.org/10.1016/j.biombioe.2019.105432.

53. Liao, Y., Koelewijn, S.-F., Van den Bossche, G., Van Aelst, J., Van den Bosch, S., Renders, T., Navare, K., Nicolaï, T., Van Aelst, K., Maesen, M., et al. (2020). A sustainable wood biorefinery for low–carbon footprint chemicals production. Science *367*, 1385–1390. https://doi.org/10.1126/science.aau1567.

54. Bartling, A.W., Stone, M.L., Hanes, R.J., Bhatt, A., Zhang, Y., Biddy, M.J., Davis, R., Kruger, J.S., Thornburg, N.E., Luterbacher, J.S., et al. (2021). Techno-economic analysis and life cycle assessment of a biorefinery utilizing reductive catalytic fractionation. Energy Environ. Sci. *14*, 4147–4168. https://doi.org/10.1039/D1EE01642C.

55. Anderson, E.M., Stone, M.L., Katahira, R., Reed, M., Muchero, W., Ramirez, K.J., Beckham, G.T., and Román-Leshkov, Y. (2019). Differences in S/G ratio in natural poplar variants do not predict catalytic depolymerization monomer yields. Nat. Commun. *10*, 2033. https://doi.org/10.1038/s41467-019-09986-1.

56. Dao Thi, H., Van Aelst, K., Van den Bosch, S., Katahira, R., Beckham, G.T., Sels, B.F., and Van Geem, K.M. (2022). Identification and quantification of lignin monomers and oligomers from reductive catalytic fractionation of pine wood with GC × GC – FID/MS. Green Chem *24*, 191–206. https://doi.org/10.1039/D1GC03822B.

57. Van Aelst, K., Van Sinay, E., Vangeel, T., Cooreman, E., Van den Bossche, G., Renders, T., Van Aelst, J., Van den Bosch, S., and Sels, B.F. (2020). Reductive catalytic fractionation of pine wood: elucidating and quantifying the molecular structures in the lignin oil. Chem. Sci. *11*, 11498–11508. https://doi.org/10.1039/d0sc04182c.

58. Lee, W.-S., Wang, Z., Wu, R.J., and Bhan, A. (2014). Selective vapor-phase hydrodeoxygenation of anisole to benzene on molybdenum carbide catalysts. J. Catal. *319*, 44–53. https://doi.org/10.1016/j.jcat.2014.07.025.

59. Prasomsri, T., Shetty, M., Murugappan, K., and Román-Leshkov, Y. (2014). Insights into the catalytic activity and surface modification of MoO_3 during the hydrodeoxygenation of lignin-derived model compounds into aromatic hydrocarbons under low hydrogen pressures. Energy Environ. Sci. *7*, 2660–2669. https://doi.org/10.1039/C4EE00890A.

60. Wong, S.S., Shu, R., Zhang, J., Liu, H., and Yan, N. (2020). Downstream processing of lignin derived feedstock into end products. Chem. Soc. Rev. *49*, 5510–5560. https://doi.org/10.1039/D0CS00134A.

61. Yang, Z., Kosir, S., Stachler, R., Shafer, L., Anderson, C., and Heyne, J.S. (2021). A GC × GC tier α combustor operability prescreening method for sustainable aviation fuel candidates. Fuel *292*, 120345. https://doi.org/10.1016/j.fuel.2021.120345.

62. Heyne, J., Rauch, B., Le Clercq, P., and Colket, M. (2021). Sustainable aviation fuel prescreening tools and procedures. Fuel *290*, 120004. https://doi.org/10.1016/j.fuel.2020.120004.

63. Heyne, J., Bell, D., Feldhausen, J., Yang, Z., and Boehm, R. (2022). Towards fuel composition and properties from two-dimensional gas chromatography with flame ionization and vacuum ultraviolet spectroscopy. Fuel *312*, 122709. https://doi.org/10.1016/j.fuel.2021.122709.

64. Funaoka, M., Kako, T., and Abe, I. (1990). Condensation of lignin during heating of wood. Wood Sci. Technol. *24*, 277–288. https://doi.org/10.1007/BF01153560.

65. Sturgeon, M.R., Kim, S., Lawrence, K., Paton, R.S., Chmely, S.C., Nimlos, M., Foust, T.D., and Beckham, G.T. (2014). A mechanistic investigation of acid-catalyzed cleavage of aryl-ether linkages: implications for lignin depolymerization in acidic environments. ACS Sustainable Chem. Eng. *2*, 472–485. https://doi.org/10.1021/sc400384w.

66. Windeisen, E., and Wegener, G. (2008). Behaviour of lignin during thermal treatments of wood. Ind. Crops Prod. *27*, 157–162. https://doi.org/10.1016/j.indcrop.2007.07.015.

67. Feldhausen, J., Bell, D.C., Yang, Z., Faulhaber, C., Boehm, R., and Heyne, J. (2022). Synthetic aromatic kerosene property prediction improvements with isomer specific characterization via GCxGC and vacuum ultraviolet spectroscopy. Fuel *326*, 125002. https://doi.org/10.1016/j.fuel.2022.125002.

68. Voigt, C., Kleine, J., Sauer, D., Moore, R.H., Bräuer, T., Le Clercq, P., Kaufmann, S., Scheibe, M., Jurkat-Witschas, T., Aigner, M., et al. (2021). Cleaner burning aviation fuels can reduce contrail cloudiness. Commun. Earth Environ. *2*, 114. https://doi.org/10.1038/s43247-021-00174-y.

69. Lee, D.S., Fahey, D.W., Skowron, A., Allen, M.R., Burkhardt, U., Chen, Q., Doherty, S.J., Freeman, S., Forster, P.M., Fuglestvedt, J., et al. (2021). The contribution of global aviation to anthropogenic climate forcing for 2000 to 2018. Atmos. Environ. (1994) *244*, 117834. https://doi.org/10.1016/j.atmosenv.2020.117834.